

# Magnetization reversal and magnetoresistance in a lateral spin-injection device

W. Y. Lee, S. Gardelis, B.-C. Choi,<sup>a)</sup> Y. B. Xu, C. G. Smith, C. H. W. Barnes, D. A. Ritchie, E. H. Linfield, and J. A. C. Bland<sup>b)</sup>  
*Cavendish Laboratory, University of Cambridge, Cambridge CB3 0HE, United Kingdom*

(Received 15 December 1998; accepted for publication 2 January 1999)

We have investigated the magnetization reversal and magnetoresistance (MR) behavior of a lateral spin-injection device. The device consists of a two-dimensional electron gas (2DEG) system in an InAs quantum well and two ferromagnetic ( $\text{Ni}_{80}\text{Fe}_{20}$ ) contacts: an injector (source) and a detector (drain). Spin-polarized electrons are injected from the first contact and propagating through InAs are collected by the second contact. By engineering the shape of the permalloy film distinct switching fields ( $H_c$ ) from the injector and the collector have been observed by scanning Kerr microscopy and MR measurements. Magneto-optic Kerr effect (MOKE) hysteresis loops demonstrate that there is a range of magnetic field (20–60 Oe), at room temperature, over which magnetization in one contact is aligned antiparallel to that in the other. The MOKE results are consistent with the variation of the magnetoresistance in the spin-injection device. © 1999 American Institute of Physics.  
[S0021-8979(99)07009-7]

## I. INTRODUCTION

One of the most interesting uses of ferromagnetic thin films is as a source of spin-polarized carriers. In particular, spin-dependent electron transport in semiconductors where ferromagnetic thin films are used to inject an imbalance of spin-polarized electrons opens an opportunity towards a new class of devices.<sup>1,2</sup> There has been intensive work on the injection of spin-polarized electrons from a ferromagnetic nonmagnetic metal, inducing interesting effects associated with spin accumulation.<sup>3,4</sup> The bipolar spin transistor by Johnson<sup>3</sup> is a device based on the injection. However, there have been few investigations on magnetotransport in ferromagnet–semiconductor systems. The possibility of spin-polarized tunneling from a ferromagnet into a semiconductor was first demonstrated by Alvarado and Renaud<sup>5</sup> who measured the degree of circular polarization of the luminescence induced by the tunneling current from a nickel tip to GaAs using a scanning transmission microscope. Similar experiments were conducted by Sueoka *et al.*<sup>6</sup> as well as Prins *et al.*<sup>7</sup> Datta and Das<sup>2</sup> proposed the idea of a spin-polarized field effect transistor (spin-FET) which would apply the spin-injection concept to ferromagnetic films on semiconductors. In such a device the current modulation results from spin precession due to spin–orbit coupling in narrow gap semiconductors while magnetic contacts are used to inject and detect spin-polarized electrons.

In this article we present the magnetization reversal related to magnetotransport in the lateral spin injection device studied previously by Gardelis *et al.*<sup>8</sup> This device is based on the idea of a spin-polarized field effect transistor. Kerr microscopy demonstrates distinct switching fields ( $H_c$ ) in the

two permalloy contacts, allowing the magnetizations of the contacts to be aligned antiparallel each other. We discuss these results in conjunction with the magnetotransport measurements in this device.

## II. EXPERIMENT

In the sample a two-dimensional electron gas (2DEG) was provided by a 15 nm wide InAs quantum well with AlSb barriers. The top AlSb barrier layer was protected from oxidation by a 5 nm GaSb layer. Ferromagnetic contacts ( $\text{Ni}_{80}\text{Fe}_{20}:A,B$ ) were deposited in the middle part of a hall bar as shown in Fig. 1. The contacts were defined by electron beam lithography and contacted to the external circuitry with a network of extended NiCr/Au contacts patterned by optical lithography. The connections of contacts *A* and *B* with the extended NiCr/Au contacts were also made from permalloy. However, we have to note that only the contacts *A* and *B* were in contact with the semiconductor surface. The rest was isolated from the surface with a layer of polyamide which was deposited on the device except for a window where the ferromagnetic contacts were located. The ferromagnetic contacts were deposited by evaporation of permalloy ( $\text{Ni}_{80}\text{Fe}_{20}$ ). The contact *A* was 5  $\mu\text{m}$  wide and the contact *B* 1  $\mu\text{m}$  wide, and both 500 Å thick, and 25 and 30  $\mu\text{m}$  long, respectively. A 200-Å-thick layer of Au was deposited on the top of the permalloy contacts in order to protect them from oxidation. The distance between two parallel contacts is 1  $\mu\text{m}$  (see Fig. 1). To ensure a good ohmic contact between the ferromagnetic contacts and the InAs layer, the top GaSb and AlSb layers were etched away selectively in the area under the contacts by dipping the sample in MF319 developer<sup>9</sup> prior to the deposition of the contacts. This process was followed by brief dipping in  $(\text{NH}_4)_2\text{S}$ . This removes any oxide from the surface of InAs under the contacts which could act as a spin scatterer due to the paramagnetic nature of oxygen. It also

<sup>a)</sup>Present address: Department of Physics, Korea Advanced Institute of Science and Technology, Taejon 305-701, Korea.

<sup>b)</sup>Electronic mail: jacbl@phy.cam.ac.uk

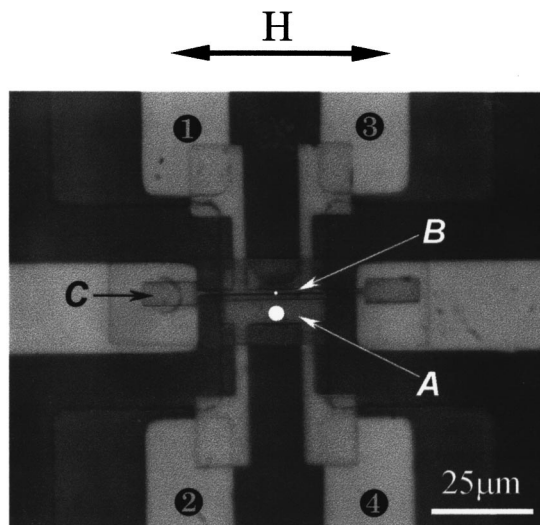


FIG. 1. An optical micrograph showing permalloy contacts *A* and *B*. The connections between the contacts *A* and *B* with the extended NiCr/Au are also shown. *C* indicates a contact pad which is a part of the structures connecting with NiCr/Au contacts for MR measurements. The dots in the center of the contacts denote approximate laser beam spot size for MOKE measurements.

passivates the InAs surface with sulphur and decelerates the oxidation process of InAs.<sup>10</sup> Within 5 min of passivation the sample was inserted in the evaporator for the deposition of the permalloy contacts. Finally, the exposed window in the polyamide was covered with cross-linked polymethylmethacrylate (PMMA).

Micron-scale magneto-optic Kerr effect (MOKE) studies have been performed to assess magnetization reversal in the two permalloy contacts. MOKE hysteresis loops were obtained at room temperature by scanning Kerr microscopy.<sup>11</sup> Two objective lenses ( $\times 20$ , numerical aperture: 0.55,  $\times 50$ , NA: 0.85) were used to focus the probing laser beam ( $\sim 4 \mu\text{m}$ ,  $\sim 1\text{-}\mu\text{m}$  spot size, respectively) on the permalloy contacts. Figure 1 displays an optical photograph showing the two permalloy contacts *A* and *B*. The connections between the contacts *A* and *B* with the extended NiCr/Au are also shown. Dots in the center of the contacts denote the approximate laser beam spot size. Magnetoresistance measurements were carried out in an applied magnetic field parallel to the 2DEG and along the long axis of the permalloy contacts *A* and *B* at a temperature varied between 300 mK and 10 K. A constant ac current of  $1 \mu\text{A}$  was applied between positions ① and ② and a voltage drop was recorded between positions ③ and ④ using lockin amplification techniques as seen in Fig. 1. The change in the magnetoresistance is defined as  $\Delta R = R_H - R_{H=0}$ , where  $R_H$  is the resistance at a given magnetic field.

### III. RESULTS AND DISCUSSION

The device was designed to operate as a spin valve. Spin-polarized electrons were injected from one ferromagnetic contact, and propagating through the InAs 2DEG, were collected from the other contact. The two permalloy contacts have been designed to show two different switching fields

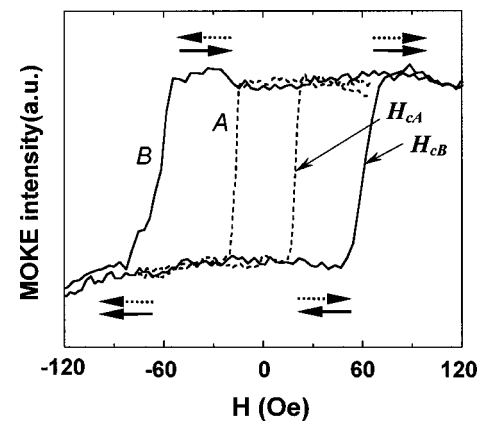


FIG. 2. Microscopic MOKE hysteresis loops for permalloy contacts *A* (dashed line) and *B* (solid line) measured by scanning Kerr microscopy at room temperature. The arrows denote parallel and antiparallel orientations of the contacts *A* and *B*, corresponding to  $H_{cA}$  and  $H_{cB}$ , respectively.

ensuring that at certain magnetic fields they are magnetized either parallel or antiparallel to each other. An examination of the magnetization reversal behavior of the two permalloy contacts has been carried out to confirm the effect using the magneto-optic Kerr effect (MOKE). Figure 2 shows microscopic MOKE hysteresis loops obtained when magnetic fields were applied parallel to the long axis of the contacts *A* and *B*, indicating that the wire axis is the easy direction of the magnetization and that there are two distinct switching fields ( $H_{cA} = 20 \text{ Oe}$ ,  $H_{cB} = 60 \text{ Oe}$ ) in the hysteresis loops for contacts *A* and *B*, respectively. These results are in qualitative agreement with previous work,<sup>12</sup> demonstrating that permalloy wires have their easy axis of magnetization along the long axis of the wire due to the magnetic shape anisotropy and a marked increase in the easy-axis switching field is observed, as the wire width decreases. This is due to buckling of the magnetization perpendicular to the wire, leading to the formation of domain walls perpendicular to the wire.<sup>12,13</sup> These walls prevent reverse domains from moving along the wire when the wire width is smaller than the buckling wavelength. It is unlikely that the domain configuration of the contacts *A* and *B* in zero applied field is a single domain due to edge domains which dominate switching behavior in ferromagnetic patterned structures.<sup>14,15</sup>

The MOKE hysteresis loops for the contacts (*A*,*B*) are compared with that of a contact pad ( $5 \times 15 \mu\text{m}^2$  *C* in Fig. 1) which is a part of the structures connecting with the NiCr/Au contacts for MR measurements and which shows a much smaller switching field ( $H_c \approx 3 \text{ Oe}$ ). Our previous work<sup>11</sup> demonstrated that a hysteresis loop from a focused beam in the center of a ferromagnetic wire represents its magnetic properties except for the edge areas, where the spatial variation in the demagnetizing field is significant due to the free poles. We also found that the junction is crucial in determining the magnetization reversal and switching field.<sup>11</sup> In fact, it was found that the switching fields at the junctions in the device, formed by the electrode ( $\text{Ni}_{80}\text{Fe}_{20}$ ) and the perpendicular arm ( $\text{Ni}_{80}\text{Fe}_{20}$ ), are smaller than those in the center of the two contacts. Nevertheless, it is clear from Fig. 2 that such a design provides the contacts (*A*,*B*) with two distinct

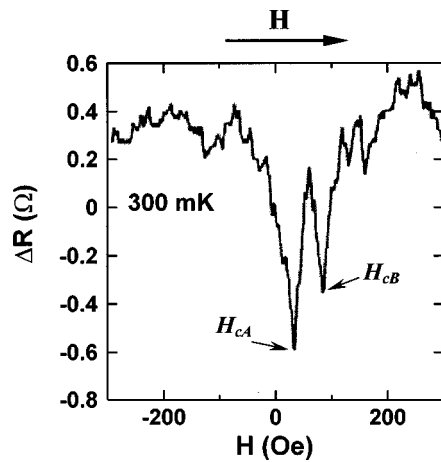


FIG. 3. Variation in the magnetoresistance ( $\Delta R$ ) between permalloy contacts *A* and *B*. The arrow shows the direction of the sweeping magnetic field.

switching fields between which the magnetization in one contact is aligned antiparallel to that in the other. In Fig. 2, the arrows represent parallel and antiparallel orientations of the magnetization of the contacts (*A*, *B*). The MOKE hysteresis results show directly that there is a range of magnetic field (20–60 Oe) in the device where the magnetization of the contacts *A* and *B* are antiparallel with respect to each other.

Next we present, in Fig. 3, the variation in the magnetoresistance ( $\Delta R$ ) of our spin injection device measured at 300 mK when a magnetic field is swept up along the long axis of the permalloy contacts. Striking peaks were found at 35 and 85 Oe, respectively. This shows the switching of the polarization of the electron spin in the device for certain magnetic fields which correspond to the switching fields of the magnetization of the two permalloy contacts.

From weak antilocalization which was observed in the four terminal near zero field magnetoresistance measurements in our InAs 2DEG system we were able to estimate a spin dephasing length ( $l_{sd}$ ) for the electrons in the device. These measurements were made on a standard Hall bar without magnetic contacts in magnetic fields applied perpendicular to the 2DEG. Weak antilocalization in such structures is caused by the spin splitting of the conduction band which is the predominant cause of spin dephasing.<sup>16</sup> Using the fitting method described in Ref. 16 we estimated the spin dephasing time ( $\tau_{sd}$ ) to be  $\sim 9$  ps. Using a mobility  $\mu = 4.9 \text{ m}^2 \text{ s}^{-1} \text{ V}^{-1}$  and an electron density  $n_s = 6 \times 10^{15} \text{ m}^{-2}$  calculated from the Shubnikov–de Haas oscillations of the four terminal magnetoresistance and an effective mass  $m = 0.04m_0$  ( $m_0$  = electron rest mass) for InAs,<sup>17</sup> the spin dephasing length ( $l_{sd}$ ) was calculated as  $1.8 \mu\text{m}$ . For the calculations we used the expression,  $l_{sd} = (l v_F \tau_s)^{1/2}$ , where  $l$  is the elastic mean free path and  $v_F$  the Fermi velocity in the system. Although the spin diffusion length is comparable to the distance ( $1 \mu\text{m}$ ) between the two permalloy contacts,  $\Delta R/R$  is only 0.2%. The most likely reason for such a small value of  $\Delta R/R$  is that the electrons leaving one contact and entering the next can have a variety of different path lengths. Thus we are measuring an average signal for electrons which have undergone different degree of precession. However,

only a small percentage of the electrons propagate without spin scattering contributing to the observed signal.

We have modeled the observed change in the magnetoresistance ( $\Delta R$ ) as follows:

$$\Delta R = \Delta R_A + \Delta R_B + \Delta R_{CA} + \Delta R_{CB} + \Delta R_S, \quad (1)$$

where  $\Delta R_A$  and  $\Delta R_B$  are the magnetoresistance changes of the permalloy contacts *A* and *B*, respectively, while  $\Delta R_{CA}$  and  $\Delta R_{CB}$  are those of the interface between the semiconductor and the contacts *A* and *B*, respectively.  $\Delta R_S$  results from electrons propagating from the first permalloy contact to the second without spin scattering. In previous work,<sup>8</sup> we have found that  $\Delta R_A$  and  $\Delta R_B$  were much smaller than  $\Delta R$ . Thus, these contributions are negligible. Therefore in order to explain the observed signal we took into account only the contributions from the interface contacts ( $\Delta R_{CA} + \Delta R_{CB}$ ) and the InAs ( $\Delta R_S$ ). Taking into account the zero-spin splitting in InAs and the fact that it is diamagnetic, the contribution from the interface contacts is a maximum when the magnetization in both ferromagnetic contacts is antiparallel to the spin orientation in the InAs 2DEG, and a minimum when the magnetization in the two ferromagnetic contacts is parallel to the spin orientation in the InAs.  $\Delta R_S$ , however, is a minimum when both permalloy contacts are magnetized parallel to each other and a maximum between the two coercive fields where the magnetization of the two contacts is antiparallel to each other. The observed signal is the sum of these two contributions.

#### IV. CONCLUSION

We have investigated the magnetization reversal and magnetoresistance in a lateral spin injection device with an InAs two-dimensional electron gas (2DEG) and two ferromagnetic ( $\text{Ni}_{80}\text{Fe}_{20}$ ) contacts placed  $1 \mu\text{m}$  apart. We found that spin-polarized electrons are injected from the first ferromagnetic contact and propagating through InAs are collected by the second contact. Magneto-optic Kerr effect (MOKE) hysteresis loops demonstrate that there is a range of magnetic field (20–60 Oe) over which the magnetization in one contact is aligned antiparallel to that in the other. The MOKE results are consistent with the variation of the magnetoresistance. There are two contributions to the magnetoresistance. The first is an interface resistance between ferromagnet and semiconductor, resulting from the zero spin splitting in InAs. The second results from spins propagating from one ferromagnetic contact to the next contact. This is a maximum between the switching fields of the two permalloy contacts.

#### ACKNOWLEDGMENTS

The authors would like to thank the EPSRC (UK), EC (Spider and Massdots Projects), Newton Trust and the Paul Instrument Fund for supporting the work. W. Y. Lee is grateful for the financial support of the British Council Korea.

<sup>1</sup>G. A. Prinz, Phys. Today **4**, 58 (1995); in *Ultrathin Magnetic Structures II*, edited by J. A. C. Bland and B. Heinrich (Springer, Berlin, 1994), Chap. 1.

<sup>2</sup>S. Datta and B. Das, Appl. Phys. Lett. **56**, 665 (1990).

- <sup>3</sup>M. Johnson, *Science* **260**, 320 (1993); *Phys. Rev. Lett.* **70**, 2142 (1993); *J. Magn. Magn. Mater.* **140-144**, 21 (1995).
- <sup>4</sup>A. Fert and S. F. Lee, *J. Magn. Magn. Mater.* **165**, 115 (1997).
- <sup>5</sup>Alvarado and Renaud, *Phys. Rev. Lett.* **68**, 1387 (1992).
- <sup>6</sup>K. Sueoka, K. Mukasa, and K. Hayakawa, *Jpn. J. Appl. Phys., Part 1* **32**, 2989 (1993).
- <sup>7</sup>M. W. J. Prins, D. L. Abraham, and H. van Kempen, *Surf. Sci.* **287/288**, 750 (1993).
- <sup>8</sup>S. Gardelis, C. G. Smith, W. Y. Lee, C. H. W. Barnes, D. A. Ritchie, E. H. Linfield, and J. A. C. Bland, in *Proceedings of the 24th International Conference on the Physics of Semiconductors*, Jerusalem, Israel, August 1998 (World Scientific), in press.
- <sup>9</sup>C. Gatzke *et al.*, *Semicond. Sci. Technol.* **13**, 399 (1998).
- <sup>10</sup>H. Oigawa *et al.*, *Jpn. J. Appl. Phys., Part 2* **30**, L322 (1991).
- <sup>11</sup>W. Y. Lee, Y. B. Xu, C. A. F. Vaz, B.-Ch. Choi, D. G. Hasko, and J. A. C. Bland, *IEEE Trans. Magn.* (submitted).
- <sup>12</sup>A. O. Adeyeye, G. Lauhoff, J. A. C. Bland, C. Daboo, D. G. Hasko, and H. Ahmed, *Appl. Phys. Lett.* **70**, 1046 (1997).
- <sup>13</sup>M. H. Kryder, K. Y. Ahn, N. J. Mazzeo, S. Schwarzzi, and S. M. Kane, *IEEE Trans. Magn.* **16**, 99 (1980).
- <sup>14</sup>K. J. Kirk, J. N. Chapman, and C. D. W. Wilkinson, *Appl. Phys. Lett.* **71**, 539 (1997).
- <sup>15</sup>S. T. Chui, *IEEE Trans. Magn.* **34**, 1000 (1998).
- <sup>16</sup>G. L. Chen, J. Han, S. Datta, and D. B. Janes, *Phys. Rev. B* **47**, 4084 (1993).
- <sup>17</sup>E. I. Rashba, *Sov. Phys. Solid State* **2**, 1109 (1960).